

# Controlled On–Off Switching of Tight-Binding Hydrogen Bonds between Model Cell Membranes and Acetylated Cellulose Surfaces

Andrey A. Gurtovenko<sup>\*,†,‡,§,||,⊥</sup> and Mikko Karttunen<sup>†,§,||,⊥</sup>

<sup>†</sup>Institute of Macromolecular Compounds, Russian Academy of Sciences, Bolshoi Prospect V.O. 31, St. Petersburg, 199004 Russia

<sup>‡</sup>Faculty of Physics, St. Petersburg State University, Ulyanovskaya str. 3, Petrodvorets, St. Petersburg, 198504 Russia

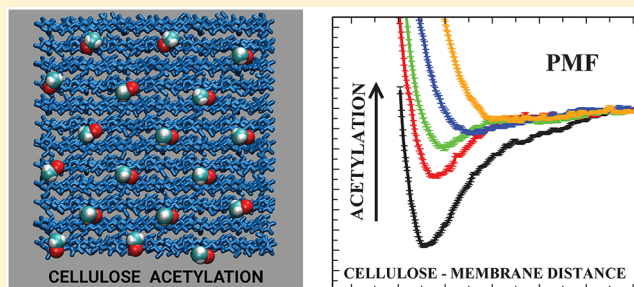
<sup>§</sup>Department of Chemistry, The University of Western Ontario, 1151 Richmond Street, London, Ontario, Canada N6A 3K7

<sup>||</sup>Department of Applied Mathematics, The University of Western Ontario, 1151 Richmond Street, London, Ontario, Canada N6A 5B7

<sup>⊥</sup>The Centre for Advanced Materials and Biomaterials Research, The University of Western Ontario, 1151 Richmond Street, London, Ontario, Canada N6A 5K7

**S** Supporting Information

**ABSTRACT:** Controlling interactions between cellulose-based materials and membranes of living cells is critical in medicine and biotechnology in, for example, wound dressing, tissue engineering, hemodialysis membranes, and drug transport. Cellulose acetylation is a widely used approach to tuning those interactions. Surprisingly, however, detailed interactions of acetylated cellulose and membranes have thus far not been characterized. Using atomistic molecular dynamics (MD) simulations, we show that the key to such control is hydrogen bonds: by tuning the number of hydrogen bonds between tissue (cell membranes) and cellulose, binding can be controlled in a precise manner. We demonstrate that the acetylation of each hydroxymethyl group reduces the free energy of cellulose–membrane binding by an order of magnitude as compared to that of pristine cellulose. Remarkably, this acetylation-induced weakening does not occur gradually and is characterized by a sharp threshold in the degree of substitution, beyond which the microscopic character of lipid–cellulose interactions changes drastically. When the degree of substitution does not exceed 0.125, the cellulose–lipid interactions are mainly driven by hydrogen bonding between cellulose’s hydroxyl groups and phosphate groups of lipid molecules. This results in the tight binding of a cellulose crystal and a lipid bilayer. Larger degrees of substitution (here, 0.25 and 0.5) prevent hydrogen bonding, leading to rather weak and unstable cellulose–bilayer binding. In this case, the lipid–cellulose binding is controlled by the interactions of lipid choline groups with hydroxyl(hydroxymethyl) groups and carbonyl groups of acetyl moieties of acetylated cellulose.



## INTRODUCTION

Cellulose-based materials are biocompatible, nontoxic, and relatively cheap. This makes them very attractive for numerous biomedical and biotechnological applications.<sup>1–4</sup> Many applications imply direct contacts of cellulose with living tissues and correspondingly with the surface of cells. Important examples include wound dressing,<sup>5</sup> biomimetic scaffolds for tissue engineering,<sup>6,7</sup> and hemodialysis membranes.<sup>8,9</sup> Therefore, the use of cellulose-based materials often requires a thorough knowledge of cellulose’s interactions with the surfaces of living cells and tuning these interactions.

Remarkably, the interactions of cellulose-based materials with plasma membranes can be critical for the biocompatibility of cellulose, as can be exemplified by undesirable interactions of cellulosic dialysis membranes with blood cells.<sup>8</sup> Recent atomic-scale computer simulations revealed the existence of the strong binding of model cell membranes (phospholipid bilayers) with the surface of a cellulose crystal, which leads to a

pronounced change in the structural properties of the bilayer leaflet in direct contact with cellulose. It was shown that such strong cellulose–phospholipid binding was mainly driven by the formation of hydrogen bonds between phosphate groups of lipids and hydroxyl (hydroxymethyl) groups of cellulose,<sup>10</sup> making these functional groups primary targets for tuning the interactions between cellulose and lipid components of cell membranes.

In general, various chemical modifications are widely used to change the surface properties of cellulose materials; these include polymer grafting, cationization (aimed at the antimicrobial activity of cellulose), esterification, and others.<sup>11</sup> The simplest way to “deactivate” hydroxyl groups on the cellulose surface is to substitute them with acetyl groups

**Received:** August 6, 2019

**Revised:** September 23, 2019

**Published:** September 25, 2019

(acetylation).<sup>12–14</sup> This reduces the ability of the cellulose surface to form hydrogen bonds with the environment, making the surface less hydrophilic. In particular, acetylation is normally employed to weaken the impact of cellulosic dialysis membranes on blood cells; dialysis membranes based on *unmodified* cellulose are not in use anymore.<sup>8,9</sup> Given the importance of acetylated cellulose, it is surprising that there is currently a complete lack of computational studies; they have the ability to reveal the interaction mechanisms and thus allow for controlled tuning of the interaction strength.

To gain molecular-level insight into the impact of acetylation on the interactions of cellulose with model cell membranes, we employ atomic-scale MD simulations. As the simplest model of the cell membrane, we consider here a bilayer built from phosphatidylcholine (PC) lipids that represents a major component of zwitterionic phospholipids in the outer leaflets of eukaryotic plasma membranes.<sup>15,16</sup> Such membranes are commonly used as model membranes in both experiments and simulations. For an in-depth discussion of membrane models, see Marrink et al.<sup>17</sup> Other main components of plasma membranes (e.g., sphingomyelin and cholesterol), being species with different hydrogen-bonding characteristics, are also of interest and can be considered in the future. We used both biased umbrella sampling and unbiased simulations to study bilayer interactions with the acetylated surface of a cellulose crystal at various values of the degree of substitution. For acetylation, we used only hydroxymethyl groups of cellulose (at the O6 position of atoms, see Figure 1) because

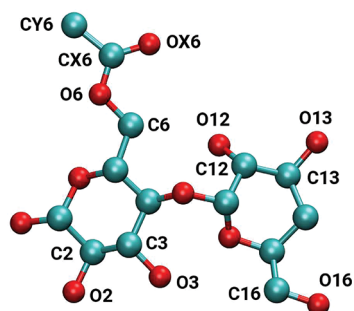


**Figure 1.** Atom numbering of a cellulose dimer with an acetylated hydroxymethyl group (C6–O6). The acetyl group is marked with the letters X and Y (CY6, OX6, and CX6). The OH groups that can be methylated are O3, O2, O6, O12, O13, and O16. Only half of these six groups can be on the surface, and thus the maximum number of OH groups per cellulose monomer available for acetylation is 1.5. The primary target for acetylation is C6–O6, and that is the only one considered here. Thus, the maximum degree of substitution here is 0.5.

these groups are the primary targets for most chemical modifications of cellulose.<sup>18</sup> We show that upon increasing acetylation, the nature of binding changes in an almost switchlike manner because of a change in the dominant binding mechanism from hydrogen bonds to nondirectional binding.

## MODELS AND METHODS

The acetylation of cellulose is characterized by the degree of substitution (DS), defined as the number of substituted groups per cellulose monomer. Each monomer has three OH groups available for substitution (Figure 1). We focus on surface modification; that is, DS cannot exceed 1.5. Because hydroxymethyl groups C6–O6 are known to be the primary targets for cellulose modification,<sup>18</sup> only these

groups were considered and DS was systematically varied from 0.0625 (every eighth O6 group acetylated) to 0.5 (each O6 group acetylated). Acetyl groups were evenly distributed over the cellulose surface. Because we consider a crystal with a relatively small surface area, it is unlikely that a random placement of acetyl groups would affect the results to a large extent. A pristine cellulose–POPC system was used as the baseline.<sup>10</sup> Table 1 shows the details.

**Table 1. Simulated Acetylated Cellulose/Lipid Membrane Systems**

system	DS <sup>a</sup>	DS-O6 <sup>b</sup>	simulation time (ns)
AC-0.0 <sup>c</sup>	0.0	0.0	600
AC-0.0625	0.0625	0.125	600
AC-0.125	0.125	0.25	600
AC-0.25	0.25	0.5	600
AC-0.5	0.5	1.0	600
AC-PMF-0.0 <sup>c</sup>	0.0	0.0	32 × 100
AC-PMF-0.0625	0.0625	0.125	32 × 100
AC-PMF-0.125	0.125	0.25	32 × 100
AC-PMF-0.25	0.25	0.5	32 × 100
AC-PMF-0.5	0.5	1.0	32 × 100

<sup>a</sup>Degree of substitution. <sup>b</sup>Degree of substitution calculated for hydroxymethyl (C6–O6) groups only. <sup>c</sup>Data taken from ref 10.

Atomic-scale MD simulations of palmitoyl-oleoyl-phosphatidylcholine (POPC) lipid bilayers interacting with acetylated cellulose surfaces were performed. The system setup was the same as in our previous study.<sup>10</sup> Briefly, the naturally occurring *1β* structure was used with a crystal consisting of 3 layers of cellulose chains with 12 chains per layer (each chain comprises 12 cellulose monomers, Figure 2).

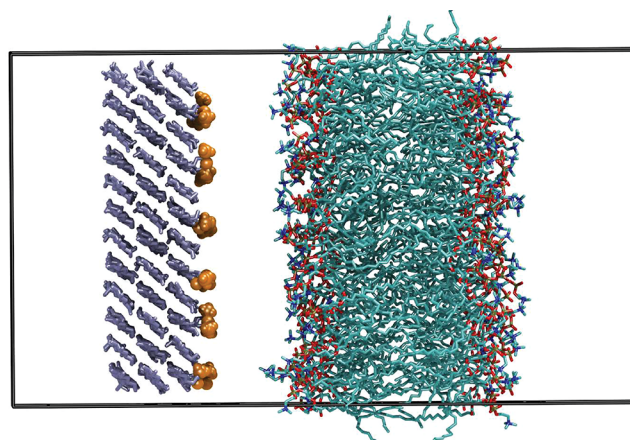


**Figure 2.** Snapshot of a POPC lipid bilayer in the vicinity of the acetylated surface of a cellulose crystal. POPC lipids are shown in cyan, red, and blue, a cellulose crystal is shown in ice blue, and acetyl functional groups on the crystal surface are shown in orange. The boundaries of a simulation box are shown by black lines. Water is not shown for clarity.

Because we focus on the interactions with the chemically modified surface of a cellulose crystal, the inner structure of the crystal was kept rigid in line with previous studies.<sup>10,19</sup> Furthermore, a cellulose crystal is indeed rigid at the length scales considered. A bilayer consisting of 148 POPC lipids was chosen to have a larger surface area compared to that of the cellulose crystal. Such a setup allows the bilayer to move with respect to the cellulose surface, thus overcoming the known limitations of lipid bilayers on a solid support.<sup>19–22</sup> Each cellulose–bilayer system was hydrated with ~12 000 water molecules, and the total number of atoms was ~65 500. The size of the cellulose bilayer has been shown to be suitable for reliable free-energy calculations.<sup>10</sup>

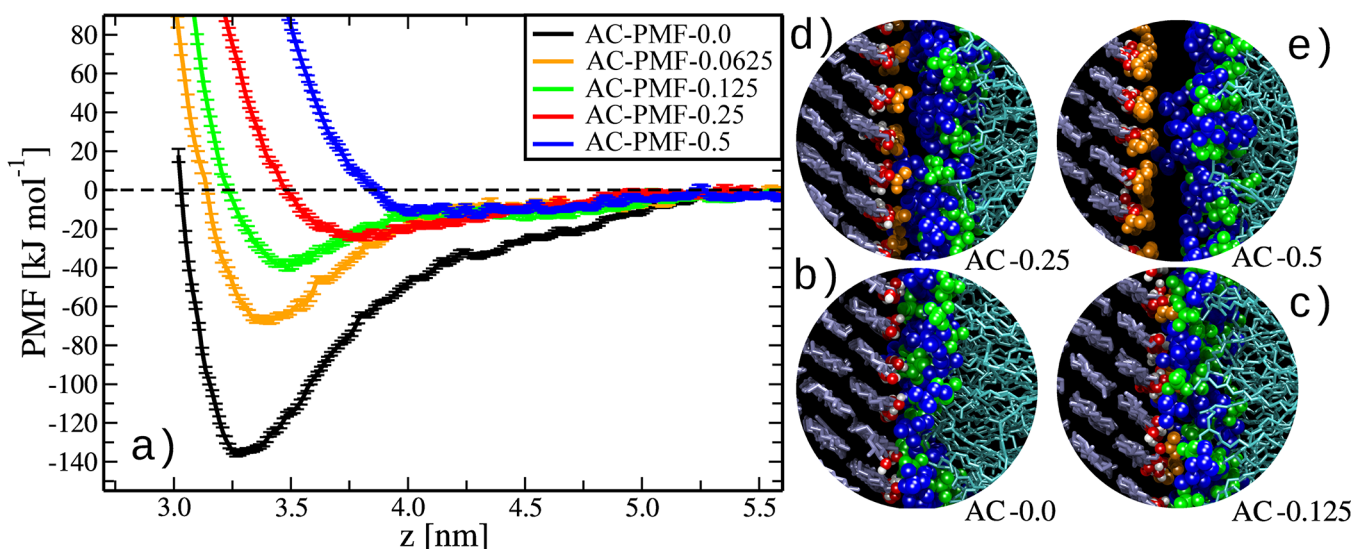


**Figure 3.** (a) Free-energy profile for the binding of a POPC lipid bilayer from aqueous solution to the acetylated surface of a cellulose crystal. The legend shows the degree of substitution (Table 1). For consistency, reaction coordinate  $z$  was chosen to be the distance along the  $z$  axis (the bilayer normal) between the centers of mass of a bilayer and an unmodified cellulose crystal. (b–e) Snapshots from the contact area. Acetylated groups of cellulose are shown in orange; hydroxyl groups of the cellulose surface are shown in red and white; choline and phosphate groups of lipids are shown in blue and green, respectively. Between  $DS = 0.0$  and  $0.125$ , hydrogen bonds dominate binding with a well-defined free-energy minimum with respect to bulk water, but at higher  $DS$ , the binding mode changes. Detailed H-bonding data is shown in Table 2, and the prevalence of different contacts is shown in Table 3.

Furthermore, possible finite size effects due to periodic boundary conditions were proven to be negligible for supported lipid bilayers with a cellulose crystal as the support.<sup>19</sup>

Extensively validated CHARMM35<sup>23,24</sup> and CHARMM36<sup>25</sup> force fields were used for cellulose and lipids, respectively. For water, the CHARMM version of the TIP3P model was used.<sup>26</sup> The structure of the crystal was kept rigid by imposing position restraints on all heavy atoms of the monosaccharide rings except hydroxyl, hydroxymethyl, and acetyl groups. All simulations were performed in the NPT ensemble ( $T = 310$  K and  $P = 1$  bar) using the Gromacs 5.1.4 simulation suite.<sup>27</sup> For pre-equilibration, we used the Berendsen scheme<sup>28</sup> for both the thermostat and barostat. For production runs, we employed the Nosé–Hoover thermostat<sup>29,30</sup> and the Parrinello–Rahman barostat.<sup>31</sup> The thermostat was applied separately to acetylated cellulose, phospholipids, and water molecules, and pressure was controlled semiisotropically. All bonds with hydrogen atoms were constrained with the P-LINCS algorithm.<sup>32</sup> Periodic boundary conditions were applied in all directions. The particle-mesh Ewald method (PME)<sup>33</sup> with a real-space cutoff of  $1.2$  nm was used for electrostatic interactions. The time step was  $2$  fs.

To evaluate the free energy of bilayer–cellulose surface binding, we used the umbrella sampling technique.<sup>34</sup> The corresponding protocol was developed and systematically tested in our previous study.<sup>10</sup> In line with ref 10, a POPC bilayer was first placed in the water phase parallel to the surface of a cellulose crystal. Because all five acetylated cellulose crystals considered in our study differ in their surface chemistry (i.e., in the value of  $DS$ , see Table 1), we chose the distance between the centers of mass (COM) of the bilayer and the unmodified cellulose crystal (in the direction perpendicular to the bilayer surface) as the reaction coordinate. This ensures that the reaction coordinate does not depend on the degree of acetylation. The initial distance between the bilayer and the crystal was set to  $5.8$  nm. The pull code supplied with the Gromacs suite<sup>27,35</sup> was used to generate starting configurations for umbrella sampling. A POPC bilayer was slowly pulled along the reaction coordinate with a velocity of  $0.0001$  nm/ps and a force constant of  $1000$  kJ mol<sup>−1</sup> nm<sup>−2</sup>. When the bilayer approached the surface of a crystal, both the velocity and force constant were increased to  $0.05$  nm/ps and  $3000$  kJ mol<sup>−1</sup> nm<sup>−2</sup>, respectively. After initial pulling, 32 windows were extracted with the reaction coordinate in the range of  $2.7$ – $5.8$  nm, which was previously

shown to be wide enough to describe the partitioning of a cellulose crystal from the water phase to the lipid/water interface of a bilayer. The spacing between windows was  $0.1$  nm. Each window was then simulated for  $100$  ns with the force constant set to  $3000$  kJ mol<sup>−1</sup> nm<sup>−2</sup>. The convergence of the PMF profiles was achieved after the first  $20$  ns so that the last  $80$  ns was used for free-energy calculations. The Gromacs implementation<sup>27,35</sup> of the weighted histogram analysis (WHAM) method<sup>36</sup> was employed to evaluate the potential of mean force (PMF). Statistical errors were estimated using bootstrapping analysis.<sup>35</sup>

The free-energy calculations were complemented with unbiased MD simulations. As starting configurations, we used generated windows for PMF calculations with the reaction coordinate equal to  $4.2$  nm. Each cellulose–bilayer system was first pre-equilibrated for  $20$  ns, and the production run for each system was extended to  $600$  ns (Table 1). This allowed us to follow unbiased binding of the POPC bilayer to the acetylated surface of a cellulose crystal. As seen in Figure S1, the initial binding (equilibration) in cellulose/lipid systems takes about  $300$  ns, so the second half of the  $600$  ns trajectory was used to study the structural properties.

## RESULTS AND DISCUSSION

The free energy of binding was computed first to determine if there are qualitative changes when the  $DS$  is varied. Figure 3 shows our main finding that binding depends on acetylation in an almost switchlike manner: the acetylation of cellulose weakens the cellulose–lipid interactions considerably, and the character of lipid–cellulose interactions changes drastically. In the following text, we focus on the mechanisms behind this behavior.

Although all of the PMF profiles in Figure 3a have a minimum, the depth decreases with increasing  $DS$ : The minimum takes values of  $136$ ,  $67$ ,  $39$ ,  $24$ , and  $12$  kJ/mol with respect to bulk water for the systems with  $DS$  equal to  $0.0$ ,  $0.0625$ ,  $0.125$ ,  $0.25$ , and  $0.5$ , respectively. Close-ups of the interfaces of four representative systems are shown in Figure 3b–e. Note that these energies correspond to the crystal surface that consists of  $12$  chains and therefore depend on the

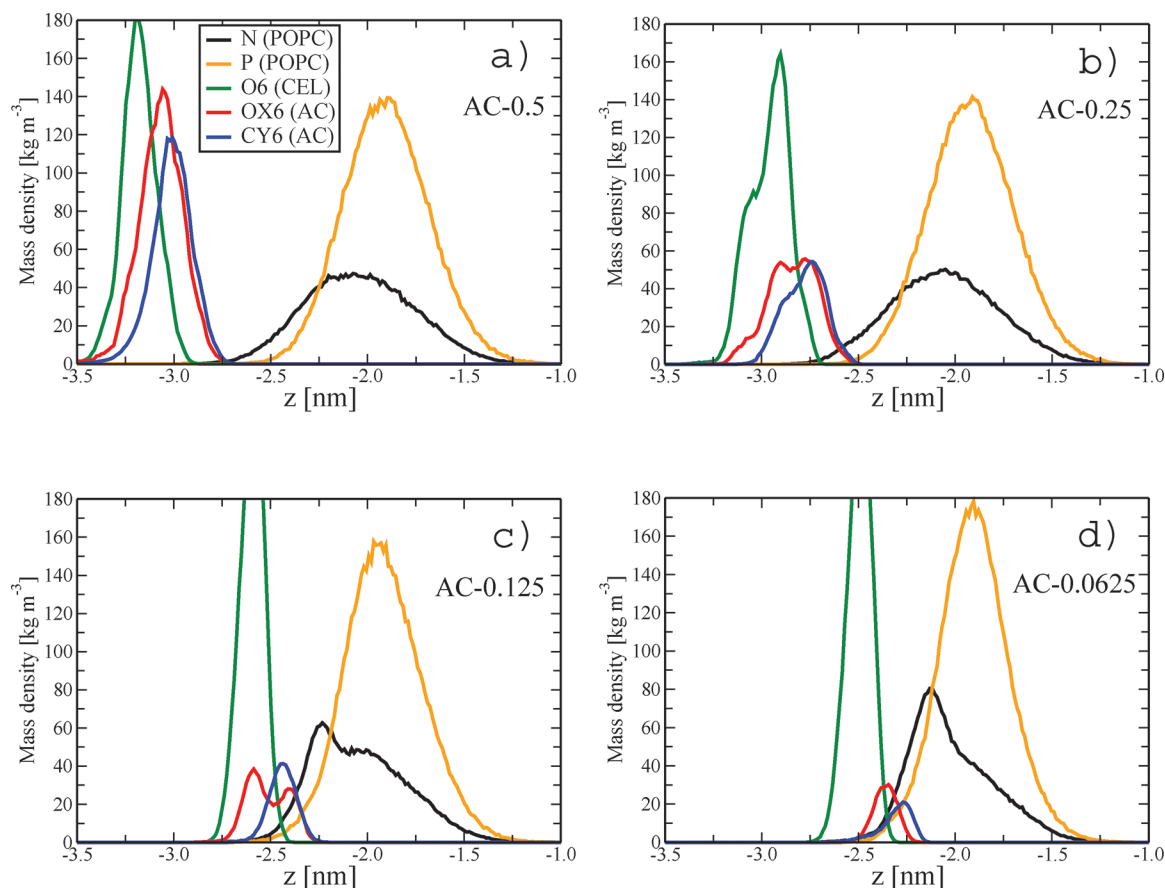


**Figure 4.** Component-wise mass density profiles for key atoms of lipid headgroups and acetylated cellulose as a function of the distance from the bilayer center ( $z = 0$ ). Shown are results for nitrogen (black lines) and phosphorus (orange lines) atoms of POPC lipids, for oxygen atoms O6 of cellulose's hydroxymethyl groups (green lines), and for the following atoms of acetyl moieties of surface-modified cellulose: carbon atoms of methyl groups (blue lines) and oxygen atoms of carbonyl groups (red lines).

surface area of a cellulose crystal. Normalizing them by the number of cellulose dimers (72) on the surface gives a more universal estimate of the free energy of binding: 1.89, 0.93, 0.54, 0.33, and 0.17 kJ/mol per cellulose dimer for the systems with DS equal to 0.0, 0.0625, 0.125, 0.25, and 0.5, respectively. For comparison, the thermal energy is about 2.5 kJ/mol. Remarkably, the acetylation of each hydroxymethyl group (C6-O6, system AC-PMF-0.5) reduces the free energy of cellulose–bilayer binding by an order of magnitude.

Figure 3a also shows that the PMF curves differ not only by the depth of the minima with respect to bulk water but also by their shapes. Indeed, the free-energy profiles can be divided into two qualitatively different groups: PMF curves with a well-defined minimum (DS equal to 0.0, 0.0625, and 0.125) and the ones characterized by a shallow profile (DS equal to 0.25 and 0.5). These two groups are well separated in terms of the positions of the free-energy minima that are located at 3.27, 3.41, 3.49, 3.76, and 4.02 nm for DS equal to 0.0, 0.0625, 0.125, 0.25, and 0.5, respectively.

Given that the length of an acetyl group along the reaction coordinate is  $\sim 0.2$  nm, the observed difference of 0.27 nm in the position of the PMF minima for systems with DS = 0.125 and 0.25 cannot be explained just by an elevated number of acyl groups on the cellulose surface: the character of the phospholipid–cellulose interactions changes when the DS exceeds a threshold value of about 0.125 (i.e., when more that

one-fourth of the hydroxymethyl groups on the cellulose surface are acetylated).

The above conclusions are also supported by unbiased simulations in which the POPC bilayer and the acetylated cellulose crystal were initially placed at a COM distance of 4.2 nm from each other (Figure S1); the data for the AC-0.0 system was taken from ref 10. In addition to structural information, such simulations can provide insight into the kinetics of cellulose–bilayer binding without any biased potentials applied. As with the free-energy calculation, all curves for the bilayer–cellulose distance can be divided into two groups: the POPC bilayer binds tightly to the acetylated surface when the DS is equal to 0.0, 0.0625, and 0.125. At larger DS values, the bilayer–cellulose binding becomes very weak. All in all, both the free energy and unbiased MD simulations clearly show that the nature of bilayer–cellulose interactions depends critically on the degree of acetylation of the cellulose surface: at DS values above 0.125, the interactions become weak and unstable. Importantly, the equilibrium cellulose–bilayer distances in unbiased simulations correlate well with the corresponding positions of the minima of PMF profiles (Figures S1 and 3a).

To obtain insight into the acetylated cellulose–bilayer interactions, the mass density profiles were computed first. The results in Figure S2 show that acetylation has an impact on the bilayer structure: at DS = 0.5, there is no overlap between lipids and cellulose, but with decreasing DS, a gradual overlap

emerges, indicating an increase in the strength of lipid–cellulose interactions. Remarkably, for the AC-0.0625 system the interactions are strong enough to induce asymmetry in the density profiles of the opposite leaflets of the bilayer (two peaks instead of one, Figure S2). Such asymmetry has also been observed for pristine cellulose.<sup>10</sup>

To gain more detailed information about the lipid–acetylated cellulose interactions, component-wise mass density profiles for the key atoms were computed: nitrogen and phosphorus atoms of the polar lipid headgroups, oxygen atoms O6 of cellulose’s hydroxymethyl groups, and carbon (CY6) and oxygen (OX6) atoms of the acetyl groups (Figure 4).

For the system with the highest degree of acetylation (DS = 0.5), the equilibrium distance between the cellulose crystal and the POPC bilayer is characterized by an almost complete lack of lipid–cellulose contacts. This picture changes when the degree of acetylation decreases: for the systems with DS ≤ 0.25, the density profiles of the choline groups (N) and carbonyl moieties of the acetyl groups (OX6) start to overlap, a signature of interactions between these groups. Remarkably, as an indication of two binding mechanisms, the density profiles for OX6 atoms develop two peaks for the AC-0.25 and AC-0.125 systems (Figure 4b,c). Furthermore, at DS equal to 0.125 and 0.0625 the N–OX6 interactions become rather strong and induce a noticeable change in the shape of the density profile of choline groups.

When DS ≤ 0.125, a new binding mechanism between the lipids’ phosphate groups and the O6 oxygen atoms of cellulose’s hydroxymethyl groups (Figure 4c) becomes dominant (observe the shifting of the peaks); in the case of pristine cellulose, the interactions between phosphate and hydroxyl groups correspond to the formation of cellulose–lipid hydrogen bonds and have been found to be critical for tight binding between the cellulose and the lipid bilayer (ref 10 and Figure S3).

Table 2 shows the average number of hydrogen bonds between the POPC phosphate groups and various hydroxyl

**Table 2. Number of Hydrogen Bonds between the Lipid Headgroups and Hydroxyl (Hydroxymethyl) Groups of Cellulose (per Cellulose Dimer)<sup>a</sup>**

	O12	O13	O6
AC-0.0	0.08 ± 0.01	0.10 ± 0.01	0.16 ± 0.01
AC-0.0625	0.02 ± 0.01	0.02 ± 0.01	0.03 ± 0.01
AC-0.125	0.01 ± 0.01	0.01 ± 0.01	0.01 ± 0.01
AC-0.25	0.0	0.0	0.0
AC-0.5	0.0	0.0	0.0

<sup>a</sup>See Figure 1 for atom numbering.

groups on the cellulose surface. The following definition was used for hydrogen bonds: the donor–acceptor distance and the hydrogen donor–acceptor angle were smaller than 0.35 nm and 30°, respectively. Remarkably, Table 2 shows that cellulose acetylation with DS equal to 0.5 and 0.25 leads to a complete lack of cellulose–bilayer hydrogen bonds. We recall that only hydroxymethyl groups C6–O6 were subject to acetylation. Nevertheless, in both AC-0.5 and AC-0.25 systems there were no hydrogen bonds between lipids, and the O12 and O13 hydroxyl groups were formed. This finding sets the minimal degree of acetylation needed to prevent tight binding between cellulose-based material and a model biological membrane: the

acetylation of just half of cellulose’s hydroxymethyl groups should suffice.

At DS ≤ 0.25, lipid–cellulose hydrogen bonds are formed (Figure 5). Similar to pristine cellulose,<sup>10</sup> the major

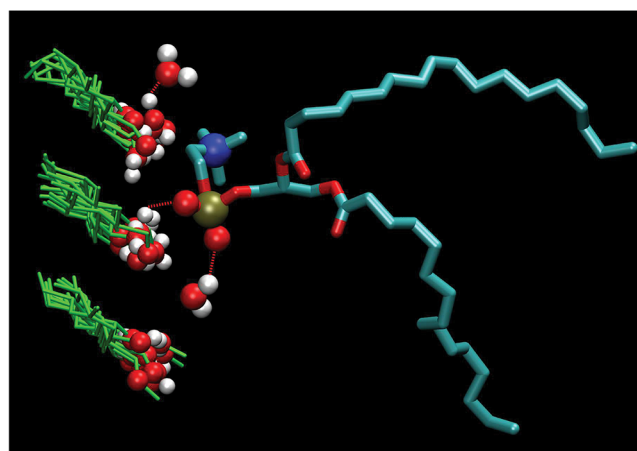


**Figure 5.** Schematic representation of hydrogen bonds formed in a cellulose–bilayer system. Shown are three types of hydrogen bonds (depicted by red dotted lines): lipid–cellulose, cellulose–water, and lipid–water bonds. Cellulose chains are shown in green, hydroxyl groups of the cellulose surface are shown in red and white, a phosphate group is shown in brown, phosphate’s oxygen atoms are shown in red, a lipid’s nitrogen atom is shown in blue, lipid acyl chains are shown in cyan, and two water molecules are shown in red and white.

contribution to these hydrogen bonds comes from cellulose’s hydroxymethyl groups (C6–O6) because they are longer and accessible to the phosphate groups of the POPC lipids (Table 2). Changes in cellulose–lipid hydrogen bonding are the underlying reason for the tight binding of a phospholipid bilayer to the cellulose surface.

For higher degrees of substitution (0.25 and 0.5), the bilayer–cellulose binding is rather weak and driven by interactions other than hydrogen bonding. To characterize them, Figure 6 shows the radial distribution functions (RDFs) of the choline groups of the POPC lipids and the various oxygen atoms on the cellulose surface: hydroxyl (O12 and O13) groups, hydroxymethyl (O6) groups, and carbonyl groups of acetyl moieties (OX6); see Figure 1 for atom numbering. As the figure shows, and consistent with the analyses above, the RDF curves can be divided into two groups: the RDFs for AC-0.25 and AC-0.5 differ considerably from the rest of the systems. In particular, the RDFs of the system with all hydroxymethyl groups acetylated (DS = 0.5) develop no sharp maxima, with the exception of a very small peak for the N–OX6 RDF (Figure 1). In turn, although one can distinguish RDF maxima for the AC-0.25, these maxima are much less pronounced compared to those for the systems with smaller degrees of acetylation. As seen in Table 3, all of these conclusions are further confirmed by the average numbers of contacts between lipid choline groups and oxygen atoms of acetylated cellulose. Thus, at DS > 0.125 the interactions of the lipid choline groups with the hydroxyl and acetyl groups of cellulose are mainly responsible for the weak binding of the lipid bilayer with the acetylated cellulose surface, providing an alternative molecular mechanism of binding, which does not involve hydrogen bonding.

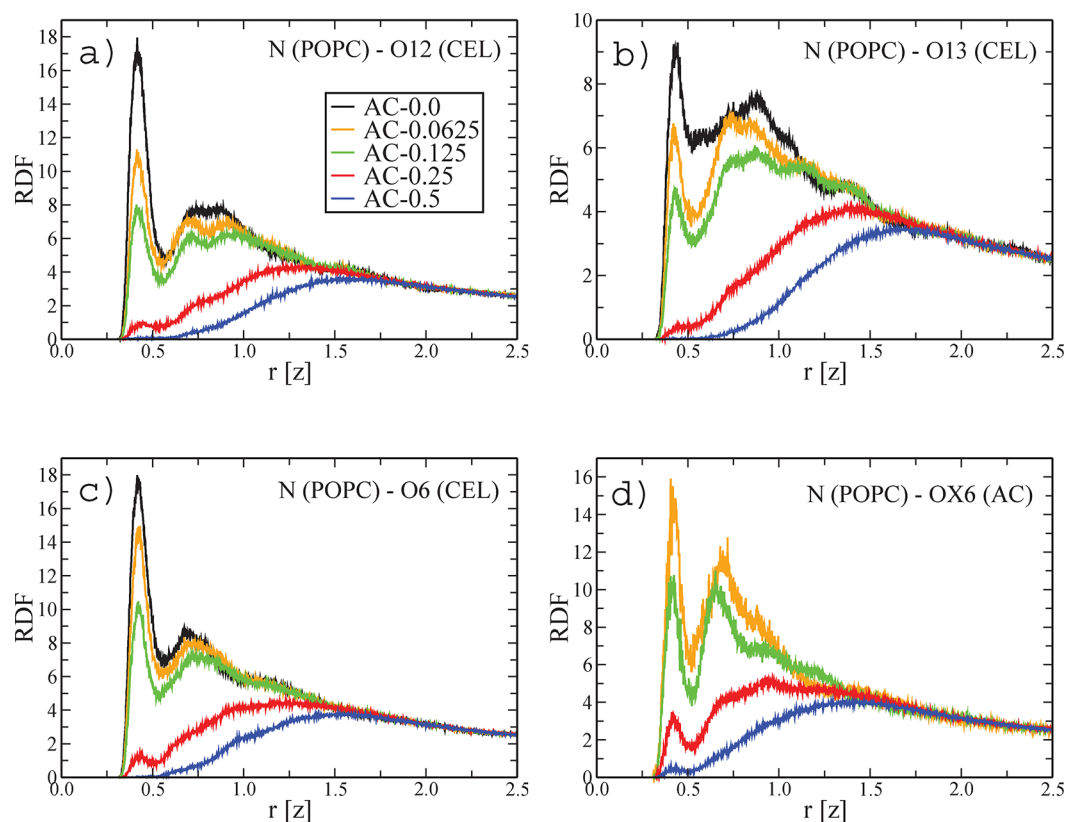


**Figure 6.** Radial distribution functions (RDFs) of nitrogen atoms of lipids' choline groups and oxygen atoms of hydroxyl (O12 and O13) and hydroxymethyl (O6) groups on the surface of a cellulose crystal as well as oxygen atoms of carbonyl groups of acetyl moieties (OX6).

**Table 3.** Number of Contacts of Nitrogen Atoms of Lipid Choline Groups with Oxygen Atoms of Hydroxyl, Hydroxymethyl, and Carbonyl Groups of Acetylated Cellulose (per Cellulose Dimer)

	O12	O13	O6	OX6
AC-0.0	0.65 ± 0.01	0.42 ± 0.01	0.71 ± 0.01	
AC-0.0625	0.42 ± 0.01	0.27 ± 0.01	0.56 ± 0.01	0.06 ± 0.01
AC-0.125	0.31 ± 0.01	0.20 ± 0.01	0.40 ± 0.01	0.08 ± 0.01
AC-0.25	0.05 ± 0.01	0.02 ± 0.01	0.06 ± 0.01	0.05 ± 0.01
AC-0.5	0.0	0.0	0.0	0.02 ± 0.01

Finally, we consider the impact of acetylated cellulose on the hydration of POPC lipid bilayers. A local level of hydration (the first hydration shell) can be characterized by the number of hydrogen bonds formed with water molecules (Figure 5). This is shown in Table 4 for both cellulose and lipid bilayers. Note that the average numbers of phosphatidylcholine–water hydrogen bonds (Table 4) are in line with previously reported computational data (around six H-bonds).<sup>37</sup> Given that the precise value of this characteristics is force-field-sensitive and

**Table 4.** Number of Hydrogen Bonds between POPC Lipids and Cellulose (per Lipid), between POPC Lipids and Water (per Lipid), and between Cellulose and Water (per Cellulose Dimer)

	lipid–cellulose	lipid–water	cellulose–water
AC-0.0	0.36 ± 0.01	6.55 ± 0.02	4.20 ± 0.02
AC-0.0625	0.06 ± 0.01	7.03 ± 0.01	4.87 ± 0.01
AC-0.125	0.03 ± 0.01	7.10 ± 0.01	4.84 ± 0.02
AC-0.25	0.0	7.19 ± 0.01	5.18 ± 0.01
AC-0.5	0.0	7.21 ± 0.01	5.02 ± 0.01

that the CHARMM36 force field gives slightly enhanced PC hydration compared to other atomic-scale force fields,<sup>38</sup> our results are in fair agreement with earlier MD studies of lipid bilayers.

For POPC bilayers, one can see a gradual increase in the number of hydrogen bonds with water when the DS increases; that is, acetylation weakens cellulose–bilayer binding. A similar trend is observed for the cellulose surface although the picture is more complex, as can be seen from the comparison of AC-0.0625 and AC-0.125 systems: in addition to the effect observed for POPC bilayers, acetylation decreases the hydrophilicity of the cellulose surface and hence lessens the ability of cellulose to form hydrogen bonds with water.

Overall, the influence of acetylated cellulose on the local hydration of lipid bilayers is relatively small. However, when it comes to the hydration of the bilayer–cellulose interfacial region, one could expect much more pronounced effects because acetylation with small DS values leads to considerably smaller cellulose–bilayer COM distances (Figures S1 and 3). To this end, the average number of water molecules in the interfacial cellulose–lipid regions was calculated, and it was found that it amounts to  $10.5 \pm 0.1$ ,  $13.9 \pm 0.2$ ,  $15.6 \pm 0.2$ ,

$23.1 \pm 0.4$ , and  $27.4 \pm 0.3$  water molecules per lipid for the AC-0.0, AC-0.0625, AC-0.125, AC-0.25, and AC-0.5 systems, respectively. Again, one can witness a gap in the hydration between the systems with DS equal to 0.0, 0.0625, and 0.125 and the rest of the systems. Remarkably, it turns out that the acetylation of each hydroxymethyl group on the surface of a cellulose crystal increases the hydration level of the interfacial cellulose–bilayer region by a factor of 3 as compared to pristine cellulose.

## CONCLUSIONS

A thorough understanding of molecular mechanisms behind the cellulose–membrane interactions is critical to the use of cellulose-based materials in medicine and biotechnology in order to be able to tune such interactions through surface modifications of cellulose. One of the simplest and most widely used modifications is acetylation, that is, the substitution of hydroxyl groups with less hydrophilic acetyl groups.

In this work, we employed both biased and unbiased atomic-scale MD simulations of phosphatidylcholine model lipid bilayers interacting with the acetylated surface of a cellulose crystal. The degree of acetylation (the number of substituted groups per cellulose monomer) was systematically varied between 0.0 and 0.5; only the hydroxymethyl groups of cellulose (Figure 1) were acetylated because these groups are often considered to be the primary targets for the chemical modification of cellulose.

Our main results are the following: We show that the free energy of cellulose–lipid bilayer binding depends on acetylation in an almost switchlike manner. We identify the physical origin of this behavior to be switching from hydrogen-bond-dominated lipid–cellulose interactions to interactions with choline groups. The acetylation of each hydroxymethyl group on the surface of a cellulose crystal reduces the free energy of cellulose–lipid bilayer binding with respect to bulk water by an order of magnitude from 1.89 to 0.17 kJ/mol per cellulose dimer for pristine cellulose and cellulose with the degree of substitution equal to 0.5, respectively. In particular, when the degree of acetylation does not exceed 0.125 (every fourth hydroxymethyl group is acetylated), the cellulose–lipid interactions are driven by hydrogen bonding between cellulose's hydroxyl and lipids' phosphate groups. These interactions are characterized by a relatively large free energy, leading to tight binding and to considerable dehydration of the lipid–cellulose interfacial region. Second, when the degree of substitution is increased to 0.25, hydrogen bonding between cellulose and lipids is blocked, leading to weak and unstable cellulose–bilayer binding. Instead of hydrogen bonds, the lipid–cellulose binding becomes controlled by the interactions of lipid choline groups with the hydroxyl(hydroxymethyl) and carbonyl groups of the acetyl moieties of acetylated cellulose. Importantly, this finding sets the minimal degree of acetylation (half of cellulose's hydroxymethyl groups) needed to avoid tight binding between cellulose-based material and model biological membranes. Finally, we showed that cellulose with a degree of acetylation of as small as 0.0625 impacts the structural properties of the bilayer leaflet next to it.

We note that all of the above conclusions are made on the basis of studying single-component phosphatidylcholine lipid bilayers. Accounting for other major lipid components of the outer leaflets of plasma membranes (such as sphingomyelin) could enhance the lipid–cellulose hydrogen bonding<sup>10</sup> and therefore shift the reported threshold degree of substitution to

larger values. However, the overall physical picture most likely remains unchanged.

All in all, our computational findings serve as a basis for the rational tuning of the interactions between cellulose-based materials and lipid components of cell membranes via cellulose acetylation. We also note that the degrees of substitution are realistic and used in applications.<sup>12</sup>

## ASSOCIATED CONTENT

### Supporting Information

The Supporting Information is available free of charge on the ACS Publications website at DOI: 10.1021/acs.langmuir.9b02453.

Time evolution of the distances between a lipid bilayer and an acetylated cellulose; mass density profiles of the systems under study; and component-wise mass density profiles for key atoms of lipids and cellulose for the system with pristine cellulose (PDF)

## AUTHOR INFORMATION

### Corresponding Author

\*E-mail: [agurtovenko@gmail.com](mailto:agurtovenko@gmail.com). Web page: [biosimu.org](http://biosimu.org). Phone: +7-812-3285601. Fax: +7-812-3286869.

### ORCID

Andrey A. Gurtovenko: 0000-0002-9834-1617

Mikko Karttunen: 0000-0002-8626-3033

### Notes

The authors declare no competing financial interest.

## ACKNOWLEDGMENTS

The authors thank A. D. Glova for his help with the acetylation of cellulose. This work was supported by the Russian Ministry of Education and Science within state contract 14.W03.31.0014 (MegaGrant). The authors acknowledge the use of the SHARCNET/Compute Canada computing facilities (Canada) and the computer cluster at the Institute of Macromolecular Compounds RAS.

## REFERENCES

- (1) Dufresne, A. Nanocellulose: a new ageless bionanomaterial. *Mater. Today* **2013**, *16*, 220–227.
- (2) Qiu, X.; Hu, S. "Smart" materials based on cellulose: a review of the preparations, properties, and applications. *Materials* **2013**, *6*, 738–781.
- (3) Almeida, A. P. C.; Canejo, J. P.; Fernandes, S. N.; Echeverria, C.; Almeida, P. L.; Godinho, M. H. Cellulose-based biomimetics and their applications. *Adv. Mater.* **2018**, *30*, 1703655.
- (4) Yang, J. S.; Li, J. F. Self-assembled cellulose materials for biomedicine: A review. *Carbohydr. Polym.* **2018**, *181*, 264–274.
- (5) Boateng, J. S.; Matthews, K. H.; Stevens, H. N. E.; Eccleston, G. M. Wound healing dressings and drug delivery systems: A review. *J. Pharm. Sci.* **2008**, *97*, 2892–2923.
- (6) Lv, X. G.; Yang, J. X.; Feng, C.; Li, Z.; Chen, S. Y.; Xie, M. K.; Huang, J. W.; Li, H. B.; Wang, H. P.; Xu, Y. M. Bacterial cellulose-based biomimetic nanofibrous scaffold with muscle cells for hollow organ tissue engineering. *ACS Biomater. Sci. Eng.* **2016**, *2*, 19–29.
- (7) O'Donnell, N.; Okkelman, I. A.; Timashev, P.; Gromovych, T. I.; Papkovsky, D. B.; Dmitriev, R. I. Cellulose-based scaffolds for fluorescence lifetime imaging-assisted tissue engineering. *Acta Biomater.* **2018**, *80*, 85–96.
- (8) Kokubo, K.; Kurihara, Y.; Kobayashi, K.; Tsukao, H.; Kobayashi, H. Evaluation of the biocompatibility of dialysis membranes. *Blood Purif.* **2015**, *40*, 293–297.

- (9) Ronco, C.; Clark, W. R. Haemodialysis membranes. *Nat. Rev. Nephrol.* **2018**, *14*, 394–410.
- (10) Gurtovenko, A. A.; Mukhamadiarov, E. I.; Kostritskii, A. Y.; Karttunen, M. Phospholipid-cellulose interactions: insight from atomistic computer simulations for understanding the impact of cellulose-based materials on plasma membranes. *J. Phys. Chem. B* **2018**, *122*, 9973–9981.
- (11) Peng, B. L.; Dhar, N.; Liu, H. L.; Tam, K. C. Chemistry and applications of nanocrystalline cellulose and its derivatives: A nanotechnology perspective. *Can. J. Chem. Eng.* **2011**, *89*, 1191–1206.
- (12) Kim, D.-Y.; Nishiyama, Y.; Kuga, S. Surface acetylation of bacterial cellulose. *Cellulose* **2002**, *9*, 361–367.
- (13) Jonoobi, M.; Harun, J.; Mathew, A. P.; Hussein, M. Z. B.; Oksman, K. Preparation of cellulose nanofibers with hydrophobic surface characteristics. *Cellulose* **2010**, *17*, 299–307.
- (14) Wang, Y.; Wang, X.; Xie, Y.; Zhang, K. Functional nanomaterials through esterification of cellulose: a review of chemistry and application. *Cellulose* **2018**, *25*, 3703–3731.
- (15) Gennis, R. B. *Biomembranes: Molecular Structure and Function*; Springer-Verlag: New York, 1989.
- (16) Voet, D.; Voet, J. G. *Biochemistry*, 3rd ed.; John Wiley & Sons: New York, 2004.
- (17) Marrink, S. J.; Corradi, V.; Souza, P. C.; Ingólfsson, H. I.; Tieleman, D. P.; Sansom, M. S. Computational Modeling of Realistic Cell Membranes. *Chem. Rev.* **2019**, *119*, 6184–6226.
- (18) Roy, D.; Semsarilar, M.; Guthrie, J. T.; Perrier, S. Cellulose modification by polymer grafting: a review. *Chem. Soc. Rev.* **2009**, *38*, 2046–2064.
- (19) Kostritskii, A. Y.; Tolmachev, D. A.; Lukasheva, N. V.; Gurtovenko, A. A. Molecular-level insight into the interaction of phospholipid bilayers with cellulose. *Langmuir* **2017**, *33*, 12793–12803.
- (20) Roark, M.; Feller, S. E. Structure and dynamics of a fluid phase bilayer on a solid support as observed by a molecular dynamics computer simulation. *Langmuir* **2008**, *24*, 12469–12473.
- (21) Xing, C. Y.; Faller, R. Interactions of lipid bilayers with supports: A coarse-grained molecular simulation study. *J. Phys. Chem. B* **2008**, *112*, 7086–7094.
- (22) Hartshorn, C. M.; Jewett, C. M.; Brozik, J. A. Molecular effects of a nanocrystalline quartz support upon planar lipid bilayers. *Langmuir* **2010**, *26*, 2609–2617.
- (23) Guvench, O.; Greene, S. N.; Kamath, G.; Brady, J. W.; Venable, R. M.; Pastor, R. W.; Mackerell, A. D. Additive empirical force field for hexopyranose monosaccharides. *J. Comput. Chem.* **2008**, *29*, 2543–2564.
- (24) Guvench, O.; Hatcher, E.; Venable, R. M.; Pastor, R. W.; MacKerell, A. D. CHARMM additive all-atom force field for glycosidic linkages between hexopyranoses. *J. Chem. Theory Comput.* **2009**, *5*, 2353–2370.
- (25) Klauda, J. B.; Venable, R. M.; Freites, J. A.; O'Connor, J. W.; Tobias, D. J.; Mondragon-Ramirez, C.; Vorobyov, I.; MacKerell, A. D.; Pastor, R. W. Update of the CHARMM all-atom additive force field for lipids: validation on six lipid types. *J. Phys. Chem. B* **2010**, *114*, 7830–7843.
- (26) MacKerell, A. D.; Bashford, D.; Bellott, M.; Dunbrack, R. L.; Evanseck, J. D.; Field, M. J.; Fischer, S.; Gao, J.; Guo, H.; Ha, S.; Joseph-McCarthy, D.; Kuchnir, L.; Kuczera, K.; Lau, F. T. K.; Mattos, C.; Michnick, S.; Ngo, T.; Nguyen, D. T.; Prodhom, B.; Reiher, W. E.; Roux, B.; Schlenkrich, M.; Smith, J. C.; Stote, R.; Straub, J.; Watanabe, M.; Wiorkiewicz-Kuczera, J.; Yin, D.; Karplus, M. All-atom empirical potential for molecular modeling and dynamics studies of proteins. *J. Phys. Chem. B* **1998**, *102*, 3586–3616.
- (27) Abraham, M. J.; Murtola, T.; Schulz, R.; Pall, S.; Smith, J. C.; Hess, B.; Lindahl, E. Gromacs: high performance molecular simulations through multi-level parallelism from laptops to supercomputers. *SoftwareX* **2015**, *1–2*, 19–25.
- (28) Berendsen, H. J. C.; Postma, J. P. M.; DiNola, A.; Haak, J. R. Molecular dynamics with coupling to an external bath. *J. Chem. Phys.* **1984**, *81*, 3684–3690.
- (29) Nosé, S. A molecular dynamics method for simulations in the canonical ensemble. *Mol. Phys.* **1984**, *52*, 255–268.
- (30) Hoover, W. G. Canonical dynamics: equilibrium phase-space distributions. *Phys. Rev. A: At., Mol., Opt. Phys.* **1985**, *31*, 1695–1697.
- (31) Parrinello, M.; Rahman, A. Polymorphic transitions in single crystals: A new molecular dynamics method. *J. Appl. Phys.* **1981**, *52*, 7182–7190.
- (32) Hess, B. P-LINCS: a parallel linear constraint solver for molecular simulation. *J. Chem. Theory Comput.* **2008**, *4*, 116–122.
- (33) Essmann, U.; Perera, L.; Berkowitz, M. L.; Darden, T.; Lee, H.; Pedersen, L. G. A smooth particle mesh Ewald method. *J. Chem. Phys.* **1995**, *103*, 8577.
- (34) Torrie, G. M.; Valleau, J. P. Nonphysical sampling distributions in Monte Carlo free-energy estimation: Umbrella sampling. *J. Comput. Phys.* **1977**, *23*, 187–199.
- (35) Hub, J. S.; de Groot, B. L.; van der Spoel, D. g\_wham - a free weighted histogram analysis implementation including robust error and autocorrelation estimates. *J. Chem. Theory Comput.* **2010**, *6*, 3713–3720.
- (36) Kumar, S.; Rosenberg, J. M.; Bouzida, D.; Swendsen, R. H.; Kollman, P. A. The weighted histogram analysis method for free-energy calculations on biomolecules. I. The method. *J. Comput. Chem.* **1992**, *13*, 1011–1021.
- (37) Pasenkiewicz-Gierula, M.; Baczynski, K.; Markiewicz, M.; Murzyn, K. Computer modelling studies of the bilayer/water interface. *Biochim. Biophys. Acta, Biomembr.* **2016**, *1858*, 2305–2321.
- (38) Pluhackova, K.; Kirsch, S. A.; Han, J.; Sun, L.; Jiang, Z.; Unruh, T.; Bockmann, R. A. A critical comparison of biomembrane force fields: structure and dynamics of model DMPC, POPC, and POPE bilayers. *J. Phys. Chem. B* **2016**, *120*, 3888–3903.